2.3.3. Kinetics

The question of Fischer–Tropsch kinetics deals with the overall reaction rate expressed by the rate of CO consumption or the rate of carbon converted to organic molecules. In the absence of CO consuming side reactions, e.g. water gas shift and Boudouard reaction, these rates are equal. Selectivity is determined by the relative rates of the various reaction steps involved in the propagation–termination sequences.

It is generally accepted that the overall rate is determined by the rate of monomer formation which is the slowest or rate determining step in the sequence. Based on the different reaction mechanisms, more detailed proposals as for the mechanism of monomer formation may be put forward and with additional assumptions on rate determining steps, expressions connecting the rate of CO consumption with the partial pressure of reactants and eventually products can be derived.

Most kinetic investigations on cobalt catalysts reports only catalyst activity or turnover numbers or they fit their experimental data to an empiric power rate law valid only in the range of their experimental conditions. These power rate laws are usually expressed in terms of the partial pressures of CO and H_2 and usually show a positive order in P_{H_2} and zero or negative order in P_{CO}.

The mechanistic approach leads to more complicated expressions of the Hougen–Watson type. These expressions are mostly based on the carbide insertion theory and have the general structure shown in equation 2–45.

$$-r_{v,CO} = \frac{k_{CO} P_{CO}^{c_1} P_{H_2}^{c_2}}{\left(1 + \sum_i C_i P_{CO}^{c_{i,CO}} P_{H_2}^{c_{i,H_2}} \left(P_{H_2O}^{c_{i,H_2O}} P_{CO_2}^{c_{i,CO_2}}\right)\right)^{c_3}} \qquad (2\text{–}45)$$

The numerator of equation 2–45 usually shows a positive order in the partial pressures of both CO and H_2. The inclusion of components in the denominator depends on assumptions made as to the structure and mechanism of formation of species adsorbed on the catalytic surface. A common simplification is to assume that only a few species are present in high

enough quantities to cause rate inhibition. These species are commonly adsorbed CO, carbon deposits and monomer which may be partially hydrogenated carbon. Expressions involving additional inhibition by dissociated H_2 (Sarup and Wojciechowski, 1989) and adsorbed water and CO_2 (Withers et al., 1990) have also been proposed.

Sarup and Wojciechowski (Sarup and Wojciechowski, 1989a) have developed several versions of the general equation based on different assumptions regarding mechanisms and the rate determining step and have performed model discrimination as well as parameter estimation by fitting experimental data from a cobalt catalyst to the models. A similar work has also been reported by Rautavuoma and van der Baan (Rautavuoma and van der Baan, 1981). Development of complex mechanistic kinetic models for the formation of alkanes and alkenes and model discrimination have been reported by Lox and Froment (Lox and Froment, 1993b) for an iron catalyst.

Complex models often lead to complicated rate expressions with a substantial number of parameters. These parameters are seldom known a priori and have to be estimated from experimental rate measurements. Rate expressions for the different models often show subtle differences in their functional dependence on the partial pressures and it is difficult to avoid statistical correlation between the parameter estimates. This makes model discrimination and accurate parameter estimation very difficult.

From this point of view Yates and Satterfield (Yates and Satterfield, 1991) have proposed a simplified expression for CO consumption with only two parameters. This expression is shown in equation 2–46. They compared this equation with experimental kinetic measurements over a cobalt catalyst in a well–mixed continous–flow slurry reactor at 493–513 K, 0.5–1.5 MPa and H_2/CO feed ratios of 1.5–3.5. They obtained good correlations between predicted and experimental data using a linearized version of the equation both for their own kinetic measurements and for kinetic data for cobalt catalysts taken from the literature.

$$-r_{v,CO} = \frac{k_{CO} P_{CO} P_{H_2}}{(1 + K_{CO} P_{CO})^2} \qquad (2\text{–}46)$$

The form of this expression with a reaction order of one for the hydrogen concentration, and a order of one for the CO concentration inside the parenthesis in the denominator implicitely assumes that adsorbed CO is the main rate inhibiting species, and that hydrogenation of a carbon atom involving two adsorbed hydrogen atoms or a secondary hydrogenation of a partially hydrogenated carbon is rate determining. This is the same as the assumption made by Rautavuoma and van der Baan (Rautavuoma and van der Baan, 1981) concerning the rate determining step although their kinetic expression is more complicated. A slightly modified version of expression 2–46 with the reaction order of 3/2 for the hydrogen concentration was reported by Huff and Kobylinski (Huff and Kobylinski, 1991) to give the best fit to their experimental data, compared with other expressions reported in the literature. Their experimental studies were conducted in a fixed bed microreactor with a cobalt catalyst over a wide range of experimental conditions.

The expression 2–46 was also found to give the best fit to experimental kinetic measurements for the Fischer–Tropsch synthesis over a commercial ruthenium catalyst compared to several other kinetic models (Dixit and Tavlarides, 1983). In some of the other expressions additional inhibition by H_2, CH_4 and H_2O was included.

2.3.4. Selectivity

The most commonly accepted mechanism for the formation of linear carbon chains in the Fischer–Tropsch synthesis is the stepwise addition of C_1 –monomer units at the terminal of a growing chain. This reaction scheme is shown in 2–47.

$$\xrightarrow{k_p} \underset{\downarrow k_t\ P_{n-1}}{L_{n-1}+M} \xrightarrow{k_p} \underset{\downarrow k_t\ P_n}{L_n+M} \xrightarrow{k_p} \underset{\downarrow k_t\ P_{n+1}}{L_{n+1}+M} \xrightarrow{k_p} \qquad (2\text{–}47)$$

At steady state the ratio between the rates of formation of products P_n and P_{n-1} can be expressed as:

$$r_n/r_{n-1} = \alpha \qquad (2\text{–}48)$$

where α is designated the probability of chain growth and is related to the rate constants of chain propagation k_p and termination k_t through expression 2–49.

$$\alpha = 1 / (1 + (k_t/k_p)) \qquad (2\text{–}49)$$

In this expression the concentration of monomer is incorporated in k_p.

If the rate constants in expression 2–49 are independent of chain length, α is also independent of chain length, and the molar selectivity, S_n, to products with n carbon atoms can be expressed as:

$$S_n = \alpha^n(1-\alpha)/\alpha \qquad (2\text{–}50)$$

This selectivity distribution is often referred to as the Schulz–Flory–Anderson distribution, and in most of the work published on Fischer–Tropsch synthesis, the authors found that the composition of the hydrocarbon fraction followed this distribution at least for products with carbon numbers in the medium range. Deviations from the Schulz–Flory distribution often observed for higher carbon numbers are most probably due to olefin readsorption (Iglesia et al., 1993).

For products with short chains deviations from the Schulz–Flory distribution are commonly observed. Especially is the observed methane selectivity higher than predicted and the ethane selectivity is lower. The reasons for these deviations are discussed in several publications e.g. (Dry, 1981; Biloen and Sachtler, 1981) and explanations such as alkene insertion, cracking and α dependent of chain length have been proposed.

From the literature published on Fischer–Tropsch mechanistic studies it can be concluded that

it is difficult to explain the selectivity of methane formation from the general propagation–termination scheme. Such an explanation is given by Huff and Kobylinski (Huff and Kobylinski, 1991) by including the probability of insertion of both C_1, C_2 and C_3 species in the growing chain. They give a satisfactory description of the observed product distribution for a cobalt catalyst using this model. At high carbon numbers their prediction coincides with the Schulz–Flory distribution using a modified expression for α. Rautavuoma and van der Baan (Rautavuoma and van der Baan, 1981) have developed a specific expression for the methane selectivity dependent on the partial pressures of H_2 and CO while the rest of the hydrocarbon products are assumed to follow the Schulz–Flory distribution.

But most commonly the kinetics of methane formation is dealt with by the use of an explicit rate expression relating the rate of methane formation to the partial pressures of H_2 and CO. These are often simple power laws, but mechanistically derived expressions of the Hougen–Watson type have also been proposed (Sarup and Wojciechowski, 1989a). Yates and Satterfield (Yates and Satterfield, 1992) have found that the observed rate of methane formation for a cobalt catalyst is well fitted by equation 2–46 which is the same as they used for CO consumption, but the parameters will of course differ.

In order to build a complete kinetic model for the Fischer–Tropsch synthesis correlations must be found between the selectivity parameters and operating conditions. For a system where primarily n–alkanes following the Schulz–Flory distribution are formed this parameter will be α.

A substantial number of investigations have been performed trying to relate selectivity to catalyst characteristics and operating conditions. For cobalt catalysts selectivity was found to vary with support, dispersion, metal loading and preparation method (Reuel and Bartholomew, 1984). Concerning the effect of operating conditions the picture is not quite clear, but it seems that selectivity is primarily a function of temperature and H_2/CO ratio (Dry, 1981). The fraction of lighter hydrocarbons increases both with increasing temperature and increasing H_2/CO ratio. There may be an additional effect of increased formation of heavier products with increasing partial pressure of CO and increasing total pressure. Yates and Satterfield (Yates and Satterfield, 1992) have observed an increase in the C_1 fraction and a

decrease in C_{10+} fraction with increasing H_2/CO ratio, but little effect of temperature and pressure on selectivity for studies on a cobalt catalyst performed in a well–mixed slurry reactor. Lox and Froment (Lox and Froment, 1993a) have investigated the kinetics of the Fischer–Tropsch reaction on an iron catalyst in a tubular reactor. They found that the growth probability α was almost independent of the total pressure and the hydrogen partial pressure, but increased with increasing CO partial pressure and decreased with increasing temperature.

Quantifications of product selectivities as functions of operating conditions may be modeled with expressions relating the selectivity parameters to temperature and partial pressures. In the simple case of n–alkanes following the Schulz–Flory distribution the parameter is α or the kinetic ratio k_t/k_p. The expressions may be empiric like the model suggested by Dictor and Bell (Dictor and Bell, 1986) who found a linear relationship between k_t/k_p and the H_2/CO ratio for an iron catalyst.

Mechanistically derived models have also been proposed. Depending on the assumed reaction mechanisms these models may show a more or less complicated relationship between selectivity parameters and the partial pressures of CO and H_2. Derivation of selectivity relations and model evaluations by fitting the expressions to experimental data have been reported by (Sarup and Wojciechowski, 1989b; Rautavuoma and van der Baan, 1981) for cobalt catalysts and (Lox and Froment, 1993b) for an iron catalyst. The model of Lox and Froment predicts an increase in the chain growth probability α both for decreasing H_2/CO ratio and increasing partial pressure of CO at constant H_2/CO ratio.

2.3.5. Kinetic expressions and parameter estimation

While the kinetic expressions reported in the literature may be more or less valid for different catalysts under varying operating conditions, the values of the parameters involved is dependent on the specific catalyst studied and on activation and pretreatment procedures. This means that the kinetic and selectivity parameters for a particular catalyst have to be determined from experimental measurements of rates and selectivities in each particular case.

Complex reaction schemes give complicated relationships between rates, selectivities and operating conditions like partial pressures and temperature. The model of Wojciechowski et al. are characterized by 9 different parameters which all are dependent on temperature (Wang and Wojciechowski, 1989). Introducing temperature dependence in the model will at least double the number of unknown parameters. This makes parameter estimation very difficult, requiring a great number of carefully planned experimental measurements with a high degree of accuracy in the analyses in order to get accurate and reliable parameter values.

A suggestion for a simpler model structure could be to use equation 2–46 (Yates and Satterfield, 1991) to describe the overall rate of CO conversion, and further, to assume that the hydrocarbon distribution follows Schulz–Flory characterized by only one parameter, α, which is mainly dependent on temperature and the H_2/CO ratio (Dry, 1981). These dependencies can be incorporated in equations 2–46 and 2–49 as shown in equations 2–51 and 2–52.

$$-r_{v,CO} = \frac{A_{CO}\, e^{-\frac{E_{CO}}{RT}} P_{CO} P_{H_2}}{(1 + A_{K,CO}\, e^{-\frac{\Delta H a_{CO}}{RT}} P_{CO})^2} \qquad (2\text{–}51)$$

$$\alpha = \frac{1}{1 + A_\alpha\, e^{-\frac{E_\alpha}{RT}} f\left(\frac{P_{H_2}}{P_{CO}}\right)} \qquad (2\text{–}52)$$

Kinetic data for the Fischer–Tropsch synthesis have been reported both from experiments conducted in fixed bed reactors and CSTR's with or without a slurry surrounding the catalyst. Generally the CSTR is preferred for kinetic investigations because it ensures uniform concentrations and temperature over the catalyst bed. This makes interpretation of data easier than for a fixed bed reactor where a more sophisticated reactor model may be needed, possibly including more or less unknown transport parameters. Gas–liquid mass transfer limitations may, however, be of importance in slurry reactors (Satterfield and Huff, 1980). Bukur et al. (Bukur et al., 1990) have compared estimated values for the rate constant of CO conversion for an iron catalyst based on data from a slurry reactor and a fixed bed reactor.

Using a plug flow model with a linear dependence between gas flow and conversion for the fixed bed reactor, (Zimmerman et al, 1989), they obtained comparable values for the rate constant calculated from measurements from the two reactors. Bukur et al. conclude their study that an isothermal fixed bed reactor may be used for evaluation of Fischer–Tropsch catalysts intended for use in slurry reactors.

If selectivities or the Schulz–Flory parameter, α, are to be determined from integral reactor experiments it must be kept in mind that selectivities may vary between different locations in the reactor because of variations in concentrations, pressure and temperature. What is measured at the outlet of an integral reactor is a continuous weighted average of possibly different Schulz–Flory distributions. The deviations from the Schulz–Flory distribution becomes, however, pronounced only for the mole fraction of hydrocarbons with more than ten carbon atoms (Lox and Froment, 1993a).

Additional problems encountered in Fischer–Tropsch kinetic investigations are the formation of high molecular waxes which may fill up the pores of the catalyst particles. This may alter the observed rates both because the concentrations of reactants and products in this liquid will differ from the gas phase concentrations, and because relative concentrations may differ due to different solubilities. This liquid will also induce an additional diffusion resistance inside the particles thus making the observed rates more dependent on catalyst particle size. This dependence of activity on particle size have been observed experimentally both for iron (Zimmerman et al., 1989) and cobalt (Post et al., 1989) catalysts. These observations are in both cases explained by strong limitations on hydrogen diffusion in liquid filled pores. Post et al. found no changes in selectivity with different particle sizes.

For gas–phase reactors like fixed bed there will be an initial period where the pores are gradually filled up with liquid and during this period the catalyst activity will not be stable. Bukur et al. (Bukur et al., 1990) observed in their fixed bed experiments a rapid loss of catalyst activity during the first 50 hours on stream. They attributed this to accumulation of high molecular–weight products in the catalyst pores and changes in the catalyst composition with time. The modest drop in activity after this period was attributed to carbon deposition and other sources of deactivation.

Huff and Satterfield (Huff and Satterfield, 1985) have, using a number of simplifying assumptions, constructed a mathematical model for the simulation of liquid accumulation in catalyst pores in an integral reactor. This model was capable of making predictions on the time required to completely fill up the first pore, as well as the fraction of pore volume occupied by liquid as a function of distance into the bed at this time. Predictions were reported at different catalyst activity, operating conditions and Schulz–Flory parameter. They obtained times to fill the first pore in the range 2–90 hours and the greatest effect was caused by the assumed carbon number distribution of the products.

3. FIXED BED PILOT REACTOR

3.1. INTRODUCTION

One main object of this work was the construction of a fully automatized fixed bed pilot reactor system to provide experimental data for reactor performance evaluations and for model development, verification and parameter estimation. The reactor system was controlled by a computer, and was equipped with measurement and data logging systems for recording of axial and radial temperature profiles, and axial concentration profiles.

The basis of the reactor design was to simulate the performance of one tube in a multitubular wall–cooled reactor under strongly exothermic reacting conditions. The principles of design of such a reactor are outlined in chapter 2.1. The tube diameter of the reactor was 2.5 cm which is in the typical range of industrial operations, but the length of the reactor tube had to be shorter than what is commonly used in industrial practice due to limitations in available laboratory space and gas supply. The reactor wall was cooled by a circulating oil system. The velocity of the oil flow in the jacket surrounding the reactor tube was kept high enough to ensure isothermal axial coolant conditions.

A general description of the pilot system is given in chapter 3.2. Further details on the reactor, analysis system, control and data acquisition system and a description of operating and experimental procedures are given in the next chapters.

The aim of the experimental part of the work was to evaluate the pilot reactor under strongly exothermic reacting conditions, and to provide data for further modeling. The Fischer–Tropsch reaction was chosen as the model reaction, and a commercial cobalt on SiO_2 catalyst supported in the form of cylindrical pellets was used in the experimental study.

3.2. GENERAL DESCRIPTION

A schematic drawing of the fixed bed pilot reactor system is shown in Figure 3–1. The unit consists of a gas feed system, the reactor unit coupled with an oil circulation system to provide control of reactor temperature, a product separation system and an on–line gas chromatograph for analysis of reactor gas phase composition. More details on the construction, including a complete part list, are given in Appendix VI.

In addition to the pilot plant reactor unit shown in Figure 3–1, the system consists of a power supply unit and a control and data acquisition system described in chapter 3.4. A description of the reactor unit is given in chapter 3.3, and the analytical system is described in chapter 3.5.

The feed system comprises two separate feed lines and a line for inert gas (N_2). Additional N_2 lines are led to the expansion tank for protection of the heating oil and to the condensers. The gases are supplied from high–pressure cylinders, and the flow rates are controlled by mass flow controllers mounted on each feed line. The feed gases are mixed after the flow controllers, and the mixture is purified and preheated to desired inlet temperature prior to entering the reactor.

Liquid and waxy products are separated from non–condensable gases using 4 high pressure condensers in series. The two first condenseres are kept at 100–150 °C to avoid solidification of the separated wax. Lower boiling products are separated in the last two water cooled condensers. The condencers are drained at regular intervals, and liquid and waxy products are stored in larger tanks. During the draining process each condenser is in turn isolated from the product stream by a programmed switching of the appropriate ball valves shown in Figure 3–1. Then liquid is forced out by applying N_2 pressure on the condenser. When a condenser is empty as can be monitored by an increase in N_2 flow, the condenser is pressurized to reactor pressure with N_2 prior to connection of the condenser to the product stream.

Reactor pressure is controlled by a pressure controller on the gas stream leaving the condensers.

The state of the reactor can be monitored by recording of temperature profiles and on–line gas phase analysis. Gas phase analyses can be taken at 10 different positions in the reactor and also of the feed and product gases by use of the stream selection valve.

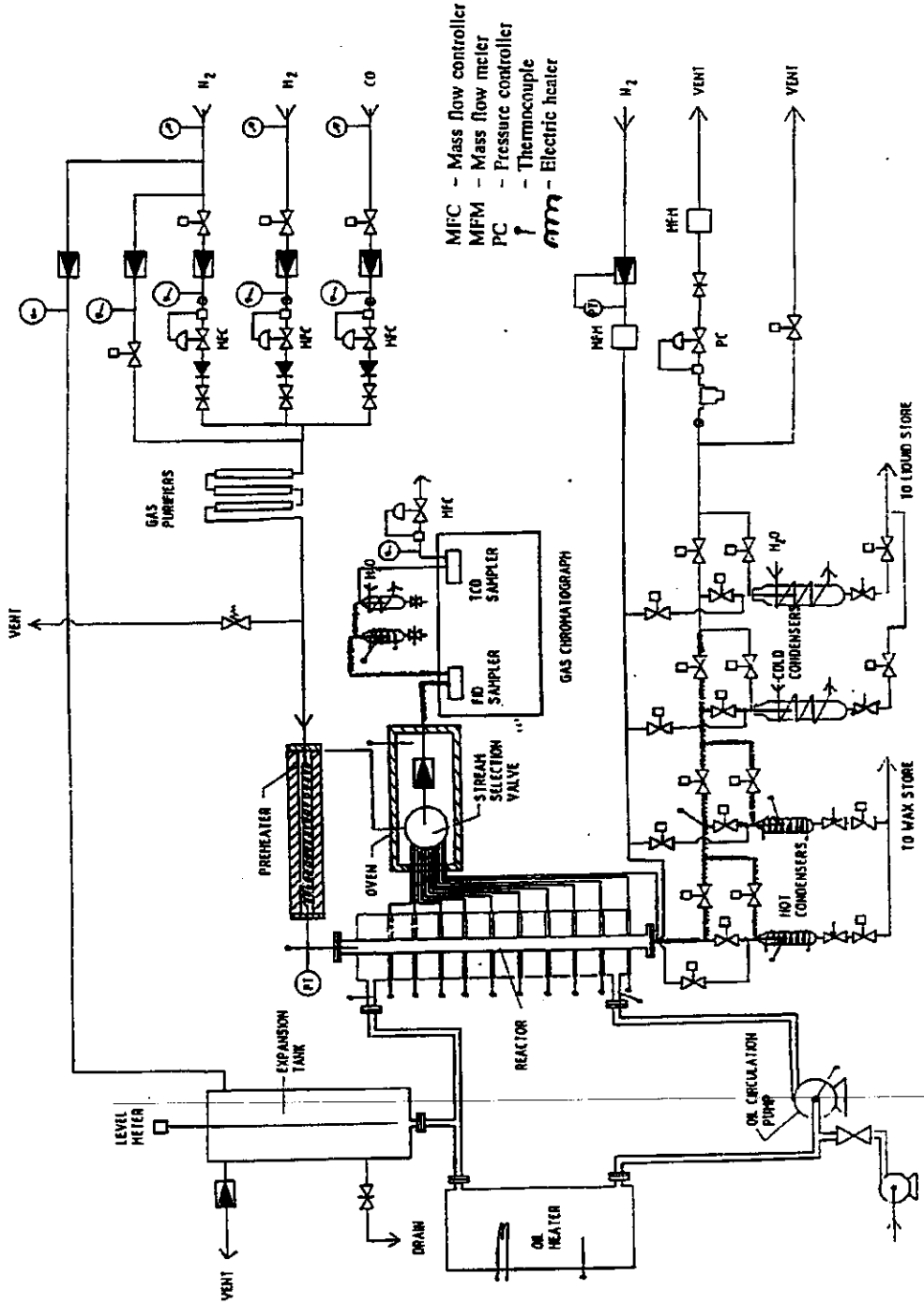

Figure 3-1. Schematic drawing of the pilot reactor system.

3.3. REACTOR AND OIL CIRCULATION SYSTEM

The reactor design is shown in Figure 3–2 and the oil circulation system and it's connection with the reactor unit is shown in Figure 3–1. The reactor materials are type 316 stainless steel and all joints are welded.

The reactor unit consists of a 25 mm inner diameter reactor tube with a wall thickness of 5 mm. Concentric with the reactor tube is a coolant jacket which is a 150 mm inner diameter tube with pipe connections at the bottom for oil inlet and at the top for oil outlet. The catalyst is held in place by a steel gauze located near the bottom of the reactor tube. The reactor is designed for a catalyst bed length of 1.5 m. The reactor tube is connected to the gas feed system and the product handling system by welded flanges and sealed by gold wire gaskets.

The inlet temperature is controlled by a thermocouple located just above the bed. Ports for insertion of gas sampling tubes and thermocouples in the bed are located at 150 mm intervals along the length of the reactor. Ports are placed at 10 different axial positions, starting 150 mm below the top of the bed and ending just above the steel gauze. At each axial position there are 4 ports which of 3 are intended for thermocouples and one for the sampling tube. The ports are constructed of bored through steel bolts welded to the reactor tube as shown in the radial cross section in Figure 3–2.

The thermocouples are 1 mm outer diameter steel jacketed and the sampling tubes are 1/16" outer diameter steel pipes. The radial positioning of thermocouples and sampling tube is shown in the radial port configuration in Figure 3–2. The thermocouples and pipes are mounted in the ports by 1/8" NPT male connectors.

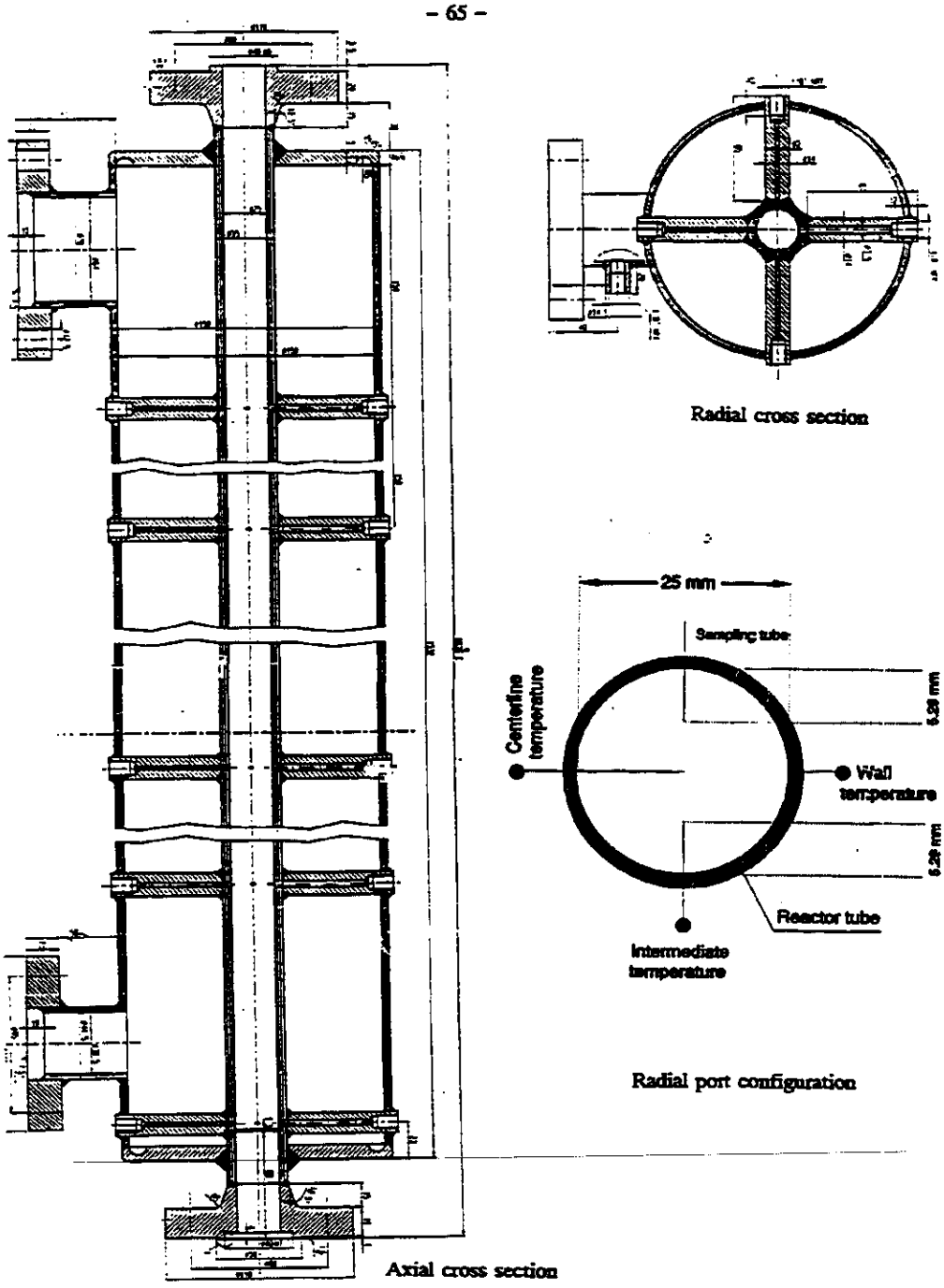

Figure 3–2. Reactor design.

The cooling jacket is connected to the oil circulation system by welded flanges and sealed by graphite gaskets. The heat transfer oil (Dowtherm G) is circulated continuously by the oil circulation pump which is a centrifugal pump designed for delivery of 250 l/min at 1 bar differential pressure. The oil was chosen because of its high maximum operating temperature (370 °C) and low vapour pressure. The high liquid velocity in the cooling jacket ensures isothermal axial conditions and good heat transfer characteristics between reactor wall and oil. The temperatures at the inlet and the outlet of the cooling jacket were monitored by thermocouples inserted in the oil stream.

To obtain reasonable heating and cooling responces, the cooling jacket and oil circulation system was partially insulated and an oil heater equipped with a 10 kW heating element was mounted in the loop. The oil heater is used to control the temperature at the inlet of the cooling jacket during operation and to bring the reactor up to operating temperature during startup.

The expansion of oil during startup heating is allowed for by the expansion tank. The tank is initially pressurized with N_2 at 5 bar to avoid boiling of the oil and to protect the oil from oxidation. Excessive pressure buildup during heating is released by a back-pressure valve.

3.4. DATA ACQUISITION AND CONTROL SYSTEM

The pilot reactor is controlled by a HP 9000 mod. 370 computer with a HP–UX operating system. Interfaced between the computer and the reactor unit is a HP–3852A data acquisition and control unit. This unit contains the necessary options for connection of thermocouples, pressure and flow measuring devices and voltage and current outputs for control of valves, heating elements and pressure and flow controllers.

The HP–3852A control unit is a programmable device with real time and multi–tasking capabilities. The low–level routines were therefore programmed in the HP–3852A language, and these tasks were performed by the HP–3852A unit. The high–level control system is located at the HP 9000 computer. This system was written in C code and runs under the X–Windows system. A block diagram of the control system is shown in Figure 3–3.

Communication between the computer and the HP–3852A is handeled by the SERVER program via the HP–IB interface. At start–up SERVER loads the low–level routines, default configuration data and default parameters and setpoints for the PID controllers from the initialization files to the control unit. Then configuration files for default valve and power supply configurations are read and the configurations are set. The oil circulation pump is started and eventually may default pressure and flow–rates be set. Finally the timer routine is started and the system is running.

During a run both configurations, PID parameters and setpoints may be changed. This can be done manually from the console or automatically at predetermined times. This is accomplished by the RUNCONTROL routine which reads commands from a file and executes them at the specified time. The product handling routine which drains the condensers are also usually started by RUNCONTROL at regular intervals.

The alarm checking and handling routines check the logged data for any unusual situations, usually if a measured data exceeds a high or low limit, and take action by alarm. If the situation is critical the unit is shut down immediately blowing the reactor content to vent and purging with N_2. Otherwise the reactor unit is shut down in a controlled manner.

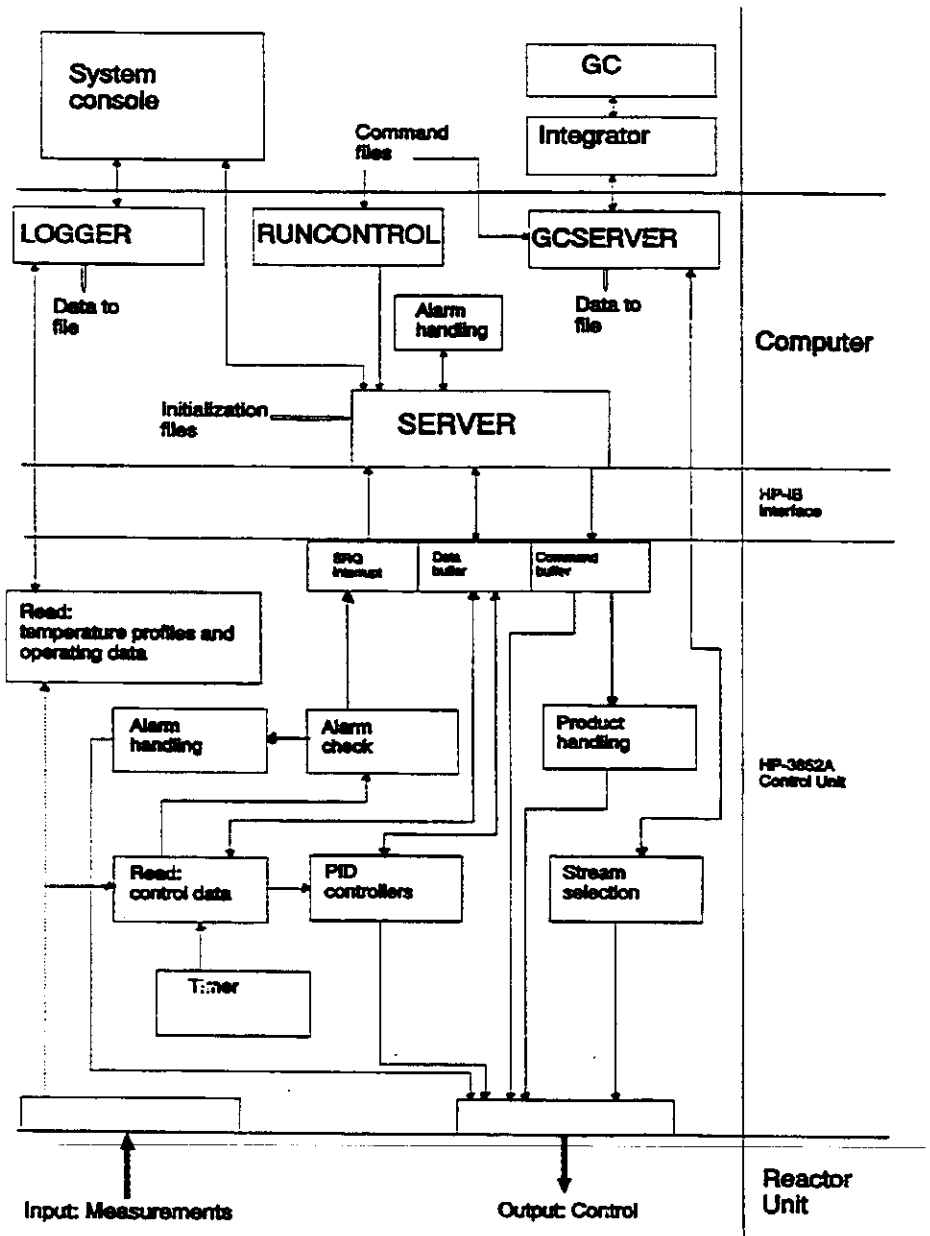

Figure 3-3. Schematic for the control system.

3.5. ANALYSIS SYSTEM

Gas sampling tubes (1/16" OD) are inserted in the bed at 10 different axial positions for on–line analysis of gas composition. The tubes are connected to a 12–port stream selection valve (Valco A6CSD 12TX), and the last two inlets of the stream selection valve are connected to sampling tubes for analysis of feed gas and exit gas composition. The outlet of the stream selection valve is connected through a pressure reducing valve to the sampling system of the gas chromatograph. Details on the gas sampling system are shown as a part of Figure 3–1.

The gas chromatograph (HP 5890A) is equipped with a flame ionization detector (FID) for the determination of the hydrocarbon distribution and a thermal conductivity detector (TCD) for the determination of nitrogen, hydrogen, carbon monoxide, carbon dioxide and methane. The hydrocarbons are separated by a wide bore capillary column (J&W DB–1) and the components determined by the TCD are separated by a packed column (Carbosieve SII). The gas chromatograph is further equipped with two gas sampling valves, one for each detector, and a cryogenic unit for low–temperature operation. Details on gas chromatograph configuration, detector calibrations and gas composition calculations are given in Appendix II.

The sample gas stream from the pilot plant first enters the FID sample valve and then a hot (100°C) condenser for the removal of waxy products and a cold condenser for removal of additional liquid products, prior to entering the TCD sample valve. These removed products may otherwise damage the Carbosieve column. The gas flow through the sampling system is controlled by a mass–flow controller at the exit. This configuration of a pressure reducing valve and a mass–flow controller makes it possible to control both the pressure and the flow in the gas sampling system. To avoid condensation of liquid products before the condensers, the tubes and valves from the reactor to the hot condenser as well as the sampling valves were kept at 250°C.

Integration, peak identification and quantifications were performed on a HP 3396A integrator connected to the gas chromatograph via the HP–IL link. This configuration also makes it possible to use the integrator as an interface between the main control system (Ch. 3.4) and

the gas chromatograph during automatic analytical sequences.

The integrator is connected to the main computer via the RS–232 link and is controlled by the GCSERVER program in the main control system (Ch. 3.4). In addition GCSERVER acts as a fileserver for the integrator, handling data transfer between the integrator and the main computer's hard–disk for the storage of analytical reports. Analytical method files for the various configurations of the integrator and gas chromatograph are also stored on the hard–disk and are loaded by GCSERVER to the integrator which configures itself and the gas chromatograph according to the data given in the method file. This includes which detector and sampling valve to be used, all temperatures and programming of the gas chromatograph and all integration and calibration parameters.

The GCSERVER program sequentially reads instructions from an input file and performs the needed action before continuing to the next command. A conformation from the environment stating that the task was succesfully completed is needed before GCSERVER continues to the next task. The commands appreciated by GCSERVER are: load a method file to the integrator, start an analytic run using the method currently loaded and wait a period or until a certain moment. In addition GCSERVER accepts requests to set the stream selection valve to a certain position thus making it possible to chose the position in the reactor from where to make a gas composition analysis. This type of request is passed on to the SERVER program and the task of positioning the valve is performed by the DAQ unit (Ch. 3.4).

Using the GCSERVER system, complex analytical tasks can be defined for automatic performance in an input file. Typically such a task would be the recording of a complete axial concentration profile using both the TCD and FID.

3.6. EXPERIMENTAL

The catalyst used in the experiments was a supported cobalt on SiO_2 catalyst, Co–0164 T 1/8" from Engelhard de Meern B.V. The catalyst was supplied in the shape of cylindrical pellets and was prereduced and stabilized with CO_2. Further details on the catalyst are given in Appendix I. The gases; CO (Norsk Hydro, 99%), H_2 (Norsk Hydro, 99.7%) and N_2 (Norsk Hydro, 99.99%) were supplied on high pressure cylinders and purified by passage through molecular sieve (Merck, 1.0 nm) prior to entering the reactor.

The reactor was loaded with catalyst up to a bed length of 1.5 m and the system was purged with N_2. The oil temperature was then brought up to 220°C while purging with N_2 to remove the adsorbed CO_2. The gas feed was then switched to H_2, and the catalyst was pretreated in H_2 at 250°C for 3 hours. Then the gas was switched back to N_2 and the oil temperature lowered to 200°C which was the starting condition for the experiments.

Starting an experiment, the flow rates and pressure were adjusted to the desired values and the composition of the feed gas was checked by GC–analysis. The oil and inlet temperatures were slowly increased to operating temperatures while continuously monitoring the temperature profile in the reactor to avoid runaway. When the catalyst activity seemed fairly stable as monitored by the temperature profile the analytical sequence and logging of temperatures were started.

Shutdown was performed by switching off CO feed and purging with H_2/N_2 for 30 min. Between the experiments the catalyst was kept in N_2 at 200°C.

4. REACTOR MODEL IMPLEMENTATION

This chapter describes the reactor simulation program. The program was written in the structured language C, and the following chapters give an overview of the essential features of the simulation system. These are the model equations, their numerical solution, the program structure and correlations and parameters used in the simulations.

4.1. MODEL EQUATIONS

In the simulation program it is assumed that the system can be described by one– or two–dimensional partial differential equations for the mass and heat balances. The program can handle one or more phases with mass and heat transfer between the phases. The fluid–phase model is based upon the two–dimensional dispersion model with radial nonuniformity in void–fraction and velocity, presented in chapter 2.2.7. The optional solid phase model is based on the diffusivity equations 2–3 and 2–4. Only steady state conditions are considered. The equations are transformed to a dimensionless form, suitable for discretization by the numerical routines. This is shown for the fluid–phase equations in 4–1 and 4–2.

Fluid phase heat balance:

$$0 = -\frac{\partial\theta}{\partial z'} + \frac{1}{Pe'_{hz}}\frac{\partial^2\theta}{\partial z'^2} + \frac{1}{Pe'_{hr}}\left[\frac{1}{r'}\frac{\partial}{\partial r'}\left(r'\frac{\partial\theta}{\partial r'}\right) + \frac{1}{\lambda_r}\frac{\partial\lambda_r}{\partial r'}\frac{\partial\theta}{\partial r'}\right] + \frac{L}{\nu\rho_g C_{pg} T_0}\rho_b\frac{(1-e)}{(1-e_0)}(-\Delta H)r_v \qquad (4\text{–}1)$$

Fluid phase mass balance:

$$0 = -\frac{\partial y_i}{\partial z'} + \frac{1}{Pe'_{mz}}\frac{\partial^2 y_i}{\partial z'^2} + \frac{1}{Pe'_{mr}}\frac{1}{r'}\frac{\partial}{\partial r'}\left(r'\frac{\partial y_i}{\partial r'}\right) + \frac{L}{\nu C_{0,i}}\rho_b\frac{(1-e)}{(1-e_0)}r_{v,i} \qquad (4\text{–}2)$$

The heat conduction boundary condition of equation 2–40b and the wall heat balance equation

The trial function for symmetric problems is shown in equation 4–3.

$$y = y(1) + (1-u^2)\sum_{i=0}^{N-1} a_i P_i(u^2) \qquad (4\text{–}3)$$

where $P_i(u^2)$ are orthogonal polynomals of degree i, a_i are the unknown constants and N is the number of interior collocation points. The residual is specified to be orthogonal to all the functions $(1-u^2)P_i(u^2)$, so the interior collocation points are located at the roots of the equation $P_N(u^2)=0$.

The fluid phase reactor domain is discretized into NR radial and NZ axial interior collocation points. Including the boundary points at r'=1, z'=0 and z'=1 this gives a total of (NR+1)·(NZ+2) algebraic equations for each PDE.

For radial collocation the Jacobi polynomals listed by Villadsen and Stewart (Villadsen and Stewart, 1967) are used to locate the collocation points. The differential operators are replaced by a weighted sum of the dependent variable y:

$$\frac{1}{r'}\frac{\partial}{\partial r'}\left(r'\frac{\partial y}{\partial r'}\right)\Bigg|_{r'=r'_j,\, z'=z'_i} = \sum_{l=1}^{NR+1} Br_{jl}\, y(z'_i, r'_l) \qquad (4\text{–}4)$$

$i=2,\ldots,NZ+1;\ j=1,\ldots,NR$

and

$$\frac{\partial y}{\partial r'}\Bigg|_{r'=r'_j,\, z'=z'_i} = \sum_{l=1}^{NR+1} Ar_{jl}\, y(z'_i, r'_l) \qquad (4\text{–}5)$$

$i=2,\ldots,NZ+1;\ j=1,\ldots,NR$

for the PDE's and the boundary conditions at r'=1. The boundary conditions at r'=0 is inherent in the symmetric trial function. Ar and Br are the elements of the matrices A and B for cylindrical geometry given by Villadsen and Stewart (Villadsen and Stewart, 1967).

The axial differential operators may be discretized similarily using matrices for non–symmetric polynomals (Finlayson, 1974). In orthogonal collocation the axial profiles are approximated using a single polynomal to cover the whole domain, and the collocation points

2–37 can be transformed to a heat transfer condition with an overall heat transfer coefficient U_c as shown in Appendix IV. Thus the same boundary conditions can be applied in the solution of equation 4–1 and 4–2 as in the traditional wall resistance models, by substituting α_w with U_c. The boundary conditions are listed in equations 2–11a to 2–11f.

The model equations 4–1 and 4–2 are also used for simulations with constant radial parameters used in traditional dispersion models. Then v is replaced by v_0, ε by ε_0, $\partial\lambda_y/\partial r$ is set to zero and λ_r is replaced by λ_{er}.

4.2. NUMERICAL SOLUTION

4.2.1. Discretization of the model equations

The reactor model equations consist, for each phase, of one partial differential equation (PDE) for the heat balance and one PDE for the mass balance of each component. Each PDE and it's boundary conditions are converted to a set of algebraic equations using the method of orthogonal collocation (Villadsen and Stewart, 1967; Finlayson, 1974; Villadsen and Michelsen, 1978).

In this method the solution is approximated by a trial function containing unknown constants which are to be adjusted according to some conditions. Using the interior collocation technique, the trial function is required to satisfy the PDE at a set of grid points called collocation points in the interior of the reactor domain, and to satisfy the boundary conditions identically. Outside the collocation points the residual between the real solution and the trial function should be tried minimized. In orthogonal collocation this is accomplished by choosing as the trial function a linear combination of orthogonal polynomals.

For radial and spherical geometry where the solutions are symmetric about the center, the dependent variable y is only a function of u^2, where u denotes a general reactor coordinate. This reduces the number of collocation points by a factor of two for problems with symmetry.

are placed at equispaced distance. This may cause problems if the profile has steep gradients in any particular region. To obtain an accurate representation of the profile, the density of collocation points should be high, which may cause numerical stability problems. It is known from numerical theory that high degree polynomals used in interpolation of smooth functions may show oscillatory behaviour, and that the Vandermonde matrices used to calculate the collocation matrices are intrinsic ill–conditioned (Press et al., 1986).

One way of solving such problems is to use collocation on finite elements (Carey and Finlayson, 1975). Another method is the use of cubic spline interpolation which is known to interpolate smoothly between the points.

Two alternative methods for axial discretization were implemented in the program. One is the standard collocation method and the other is the cubic spline interpolation method described in Appendix V. This method has no restrictions on the location or on the number of gridpoints.

The two methods gave virtually identical simulation results for relatively unsevere conditions. This was the case for simulations at the conditions used in the experimental study, using the kinetic and heat transfer parameters given in chapter 5. The number of axial gridpoints should be kept between approximately 8 – 15 for the collocation method. Above this range the method tended to be numerically unstable even at low severity, showing oscillations or failing to converge. The spline method turned out to be more stable, being able to obtain steady state solutions at more severe conditions, e.g. higher temperatures, requiring more axial gridpoints.

If the pellet equation is included in the model, it is discretized by orthogonal collocation in the same manner as for the radial collocation. The collocation points are determined using Jacobi polynomals for spherical geometry. The collocation matrices are given by Villadsen and Stewart (Villadsen and Stewart, 1967).